Article

Application of Trimethylgermanyl-Substituted Bisphosphine Ligands with Enhanced Dispersion Interactions to Copper-Catalyzed Hydrobo-ration of Disubstituted Alkenes

Yumeng Xi, Bo Su, Xiaotian Qi, Shayun Pedram, Peng Liu, and John F. Hartwig

J. Am. Chem. Soc., **Just Accepted Manuscript** • DOI: 10.1021/jacs.0c08746 • Publication Date (Web): 22 Sep 2020

Application of Trimethylgermanyl-Substituted Bisphosphine Ligands with Enhanced Dispersion Interactions to Copper-Catalyzed Hydroboration of Disubstituted Alkenes

Yumeng Xi,[a,b,†,‡] Bo Su,[a,†,#] Xiaotian Qi,[c] Shayun Pedram,[a] Peng Liu,*[,c] and John F. Hartwig*[,a,b]

[a]Department of Chemistry, University of California, Berkeley, CA 94720, United States

[b]Division of Chemical Sciences, Lawrence Berkeley National Laboratory, Berkeley, CA 94720, United States

[c]Department of Chemistry, University of Pittsburgh, Pittsburgh, Pennsylvania 15260, United States

[‡]Present Address: Materials Research Laboratory, University of California, Santa Barbara, CA 93106, United States

[#]Present Address: College of Pharmacy, Nankai University, Tianjin, 300071, China

[†]These authors contribute equally to this work

ABSTRACT: We report the incorporation of large substituents based on heavy main group elements that are atypical in ligand architectures to enhance dispersion interactions and, thereby, enhance enantioselectivity. Specifically, we prepared the chiral biaryl bisphosphine ligand (TMG-SYNPHOS) containing 3,5-bis(trimethylgermanyl)phenyl groups on phosphorus and applied this ligand to the challenging problem of enantioselective hydrofunctionalization reactions of 1,1-disubtituted alkenes. Indeed, TMG-SYNPHOS forms a copper complex that catalyzes hydroboration of 1,1-disubtituted alkenes with high levels of enantioselectivity, even when the two substituents are both primary alkyl groups. In addition, copper catalysts bearing ligands possessing germanyl groups were much more active for hydroboration than one derived from DTBM-SEGPHOS, a ligand containing 2,5-di-*tert*-butyl groups and widely used for copper-catalyzed hydrofunctionalization. This observation led to the identification of DTMGM-SEGPHOS, a bisphosphine ligand bearing 3,5-bis(trimethylgermanyl)-4-methoxyphenyl groups as the substituents on the phosphorus, as a new ligand that forms a highly active catalyst for hydroboration of unactivated 1,2-disubstituted alkenes, a class of substrates that has not readily undergone copper-catalyzed hydroboration previously. Computational studies revealed that the enantioselectivity and catalytic efficiency of the germanyl-substituted ligands is higher than that of the silyl and *tert*-butyl substituted analogs because of attractive dispersion interactions between the bulky trimethylgermanyl groups on the ancillary ligand and the alkene substrate and that Pauli repulsive interactions tended to decrease enantioselectivity.

1. INTRODUCTION

The enantioselectivity of reactions of prochiral substrates catalyzed by transition-metal complexes typically requires the metal-ligand system to distinguish between two substituents on the substrate. This distinction is most commonly thought to result from coordination of a functional group on one substituent to the metal, or by greater steric repulsion between one of the substituents and the ligands, often depicted in "quadrant diagrams."[1] Thus, the differentiation between two substituents that are similar in steric properties and lack a functional group, such as two primary alkyl groups, can be particularly challenging to achieve.

Some of the most effective phosphine ligands for enantioselective chemistry contain bulky tertiary alkyl groups in the 3,5-positions of phosphine-bound aryl groups.[2-3] However, selectivities with such ligands for many reactions are low, even after varying other reaction parameters. Recent reports[4-5] from one of our groups provided evidence that attractive dispersion interactions,[6-7] rather than repulsive steric interactions, between bulky alkyl substituents on a ligand and the substrate can increase reaction rates.[8-15] However, ligands that can increase enantioselectivity by enhanced attractive C-H–H-C dispersion intereactions are lacking.[16] Although attractive C-H–π interactions[17-18] are often invoked to rationalize selectivity, we conjectured that C-H–H-C dispersion interactions involving phosphine ligands could be modulated to increase the enantioselectivity of certain reactions that have occurred with moderate stereoselectivity previously. More specificially, we wondered whether changing the elements within substituents (e.g. *tert*-butyl groups) to heavier main-group elements could be a modular approach to enhance the attractive dispersion interactions by tuning the distance of the C-H–H-C pairs, thereby leading to improved enantioselectivities.

Heavy main-group elements have large covalent radii, thereby forming longer covalent bonds than their light congeners. Due to this feature, new reactivity of complexes containing these heavy elements has been explored extensively,[19] but their use as simple substituents to modulate the reactivity or selectivity of a catalyst has been limited. We envisioned that the attractive dispersion between the substrate and substituents containing such elements, such as trimethylsilyl and trimethylgermanyl groups, would be larger than those between the substrate and hydrocarbyl substituents, such as *tert*-butyl groups, because the main-group substituents are larger in volume. This change could ultimately lead to a catalyst that is highly active and enantioselective for reactions of 1,1-disubstituted alkenes, such as hydroboration.

Scheme 1. Development of trimethylgermanyl-substituted ligands for copper-catalyzed hydroboration of 1,1-disubstituted alkenes

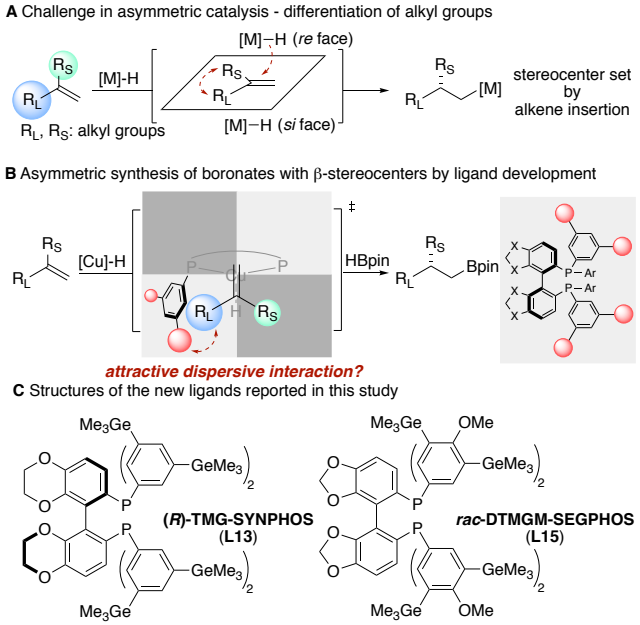

The utility of 3,5-disubstituted biaryl bisphosphines for enantioselective hydroboration and the the unsolved problem of conducting enantioselective reactions of 1,1-disubstituted alkenes that must differentiate between two alkyl substituents (Scheme 1A, 1B) led us to assess this approach for developing ligands for the asymmetric hydroborations of 1,1-disubtituted alkenes. Such reactions are particularly valuable because they form enantioenriched products that can readily undergo reactions to afford a series of functionalized molecules with β-sterogenic centers.

Although hydroboration of 1,1-aryl,alkyl-disubstituted alkenes has occurred with high levels of enantiocontrol (>95:5 er),[20-22] the hydroboration of 1,1-alkyl,alkyl-disubstituted alkenes in which the alkyl groups are similar in size has generally occurred with low enantioselectivity.[20-23] For example, Yun and co-workers reported a copper system that catalyzed the hydroboration of 1,1-disubstituted alkenes that contain one primary alkyl group and one secondary alkyl group with high enantioselectivity,[24] but the same reaction of 1,1-disubstituted alkenes that contain two different primary alkyl groups occurred with only modest enantioselectivity (below 85:15 er). In fact, examples of any type of hydrofunctionalization of 1,1-disubstituted alkenes that bear two different primary alkyl groups with high enantioselectivity[25] are rare.[26-30]

Herein, we report two new bisphosphine ligands (*R*)-TMG-SYNPHOS (**L13**) and DTMGM-SEGPHOS (**L15**) that are based on the principle of enhancing attractive interactions (Scheme 1C). They bear trimethylgermanyl groups at the 3- and 5-positions of the phenyl groups on the phosphorus of the ligand, and they generate more active and selective copper catalysts for hydroboration, including enantioselective hydroboration of 1,1-disubstituted alkenes that bear two different primary alkyl groups over the most selective current catalysts, which are derived from DTBM-SEGPHOS. These trimethylgermanyl-substituted catalysts are more active than those formed from DTBM-SEGPHOS, and combining the 3,5-trimethylgermanyl groups with the 4-methoxy donor in the form of DTMGM-SEGPHOS created a catalyst for the hydroboration of unactivated internal alkenes that reacts in much higher yields than catalysts formed from DTBM-SEGPHOS. Computational studies strongly suggest that the higher enantioselectivity and catalytic efficiency of the germanyl-substituted ligands than of the silyl and *tert*-butyl substituted analogs result from attractive dispersion interactions, not repulsive steric interactions, between the bulky trimethylgermanyl groups on the ancillary ligand and the alkene .

2. RESULTS AND DISCUSSION

2.1 Design of new bisphosphine ligands for asymmetric hydroboration of 1,1-disubstituted alkenes. To develop a metal-ligand system that catalyzes the hydroboration of 1,1-disubstituted alkenes bearing two primary alkyl groups with high levels of enantioselectivity, we sought to modify the aryl substituents on the phosphorus of DTBM-SEGPHOS. For many reactions catalyzed by complexes with axially chiral biaryl bisphosphines, larger substituents on the P-aryl groups lead to higher enantioselectivity. Previous studies on copper-catalyzed enantioselective hydroboration have shown that the large substituents on the phosphorus-bound aryl rings increase enantioselectivity[31] and a rhodium complex containing the trimethylsilyl-substituted ligand (*S*)-TMS-SEGPHOS catalyzed enantioseletive silylations of C-H bonds with higher selectivities than that with related ligands containing *tert*-butyl groups.[32-33] We postulated that trimethylgermanyl group, which has a larger volume than trimethylsilyl and *tert*-butyl groups because carbon-germanium bonds are longer than carbon-carbon and carbon-silicon bonds, would lead to a system that could catalyze the hydroboration of 1,1-disubstituted alkenes with high enantioselectivity.

To test this hypothesis, we conducted density functional theory (DFT) calculations on the transition states of hydrocupration of 2-methyl-1-pentene (**1**) with copper hydride complexes ligated by a series of SEGPHOS-derived ligands containing different 3- and 5-substituents on the *P*-aryl groups (Scheme 2). The olefin insertion was shown to be the enantioselectivity-determining step of the hydroboration in our previous report.[31] The difference in computed activation free energies ($\Delta\Delta G^{\ddagger}$) between transition states leading to the major and minor enantiomeric products increased as the size of the substituents at the 3- and 5-positions increased from *tert*-butyl to trimethylsilyl and trimethylgermanyl. In addition, the computed barrier of hydrocupration ($\Delta G^{\ddagger}$) decreases when a bulkier substituent was placed on the ligand. This suggests that the greater enantioselectivity of the reaction with the (*S*)-TMG-SEGPHOS ligand is a result of stabilizing the transition state leading to the major enantiomer (**TS-3A**), rather than destabilizing the disfavored transition state (**TS-3B**) by steric effects (see later for detailed computational analysis of the origin of the ligand effects).

Scheme 2. DFT calculations of reactivity and enantioselectivity of olefin hydrocupuration with copper hydride complexes ligated by SEGPHOS-derived ligands. All energies are in kcal/mol.

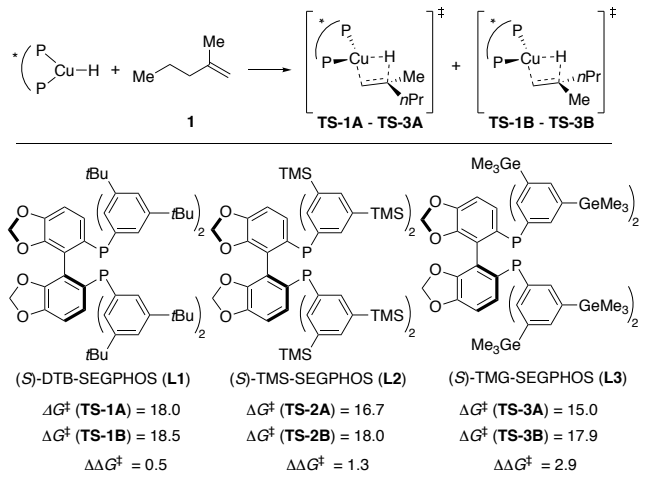

Synthesis of (*R*)-TMG-SYNPHOS and (*R*)-TMS-SYNPHOS. The trend of enantioselectivity predicted by DFT calculations prompted us to devise a synthetic route to prepare ligands that contain 3,5-trimethylgermanyl groups. We chose to prepare SYNPHOS derivatives first, instead of SEGPHOS derivatives, because it is convenient to access enantioenriched SYNPHOS ligands by laboratory resolution. Ligands that contain 3,5-trimethylstannyl groups would have the potential to create catalysts that are more active and enantioselective than ligands that contain 3,5-trimethylgermanyl groups. However, the high toxicity of organostannane compounds and potential modification of the ligand by reactions at the C-Sn bonds led us to pursue the synthesis of germanyl-substituted ligands instead of stannyl-substituted ligands.

Scheme 3. Synthesis of (*R*)-TMG-SYNPHOS (L13) and (*R*)-TMS-SYNPHOS (L12)

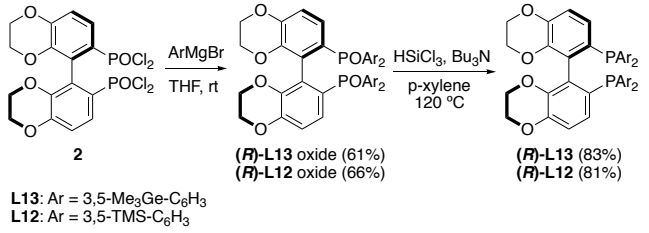

As depicted in Scheme 3, (*R*)-TMG-SYNPHOS was prepared in just two steps starting from known intermediates.[34-35] The Grignard reaction between (*R*)-(2,2',3,3'-tetrahydro-[5,5'-bibenzo[*b*][1,4]dioxine]-6,6'-diyl)bisphosphonic dichloride (**2**), which was synthesized in three steps,[34] and the corresponding aryl magnesium bromide, which was generated from 3,5-bis(trimethylgermanyl)phenyl bromide[36] afforded (*R*)-TMG-SYNPHOS oxide in 61% yield. (*R*)-TMS-SYNPHOS oxide was prepared in 66% yield by an analogous route. Reduction of the phosphine oxide in the presence of trichlorosilane and tributylamine afforded the corresponding phosphines in 81-83% yield. The overall yields from the two-step syntheses were close to 50%. Based on this procedure, a total of one gram of each ligand was prepared.

Table 1. Evaluation of ligands for enantioselective hydroboration of 1,1-disubstituted alkene 3a[a]

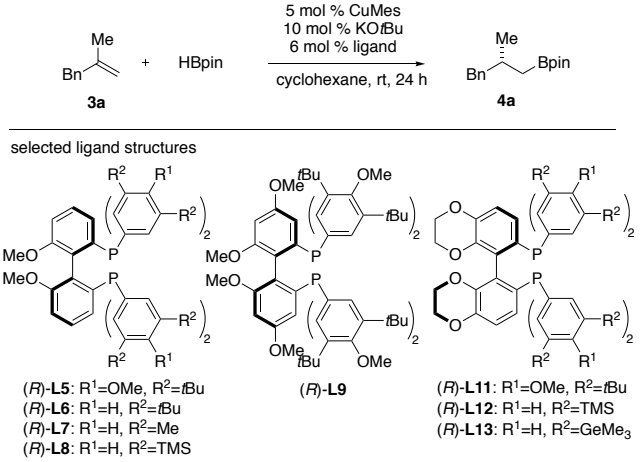

entry	ligand	T	yield[b] (%)	er
1	(*S*)-DTBM-SEGPHOS (**L4**)	rt	93	17:83
2	(*R*)-DTBM-MeOBIPHEP (**L5**)	rt	81	80:20
3	(*S*)-DTB-MeOBIPHEP (**L6**)	rt	95	18:82
4	(*R*)-DM-MeOBIPHEP (**L7**)	rt	<5	-
5	(*R*)-TMS-MeOBIPHEP (**L8**)	rt	83	86:14
6	(*R*)-DTBM-garphos (**L9**)	rt	81	78:22
7	(*R*)-DTBM-BINAP (**L10**)	rt	91	79:21
8	(*R*)-DTBM-SYNPHOS (**L11**)	rt	93	85:15
9	(*R*)-TMS-SYNPHOS (**L12**)	rt	87	88:12
10[c]	(*R*)-TMS-SYNPHOS (**L12**)	-15 °C	48	92:8
11[c]	(*R*)-TMG-SYNPHOS (**L13**)	-15 °C	93	94:6
12[c]	(*S*)-DTBM-SEGPHOS (**L4**)	-15 °C	<5	-

[a]Reaction conditions: **3a** (0.25 mmol, 2.5 equiv), HBpin (0.10 mmol, 1 equiv), CuMes (5 mol %), KO*t*Bu (10 mol %) and ligand (6 mol %) in cyclohexane (0.15 mL), rt, 24 h; [b]Determined by GC against dodecane as an internal standard; [c]**3a** (0.2 mmol), HBpin (0.24 mmol, 1.2 equiv), CuMes (5 mol %), KO*t*Bu (10 mol %) and ligand (5 mol %) in decalin (0.14 mL), 72 h.

Effects of the ligands on enantioselectivity. Initial studies to evaluate the effect of a series of axially chiral biaryl bisphosphines on the enantioselectivity of the copper-catalyzed hydroboration are shown in Table 1. These reactions were conducted with 2-methyl-1-phenylpropene (**3a**), which contains a benzyl and a methyl group on the olefin. Yun reported that the enantiomeric ratio of the reaction of **3a** under conditions they developed with (*S*)-DTBM-SEGPHOS as ligand was only 82:18.[24] This prior result implies that the catalyst formed from (*S*)-DTBM-SEGPHOS inadequately differentiates a benzyl from a methyl group to achieve high enantioselectivity. We repeated this reaction with the conditions of 5 mol % mesitylcopper, 10 mol % potassium *tert*-butoxide, and 5.5 mol % (*S*)-DTBM-SEGPHOS and obtained the hydroboration product with 83:17 er (entry 1).[37]

The effect of the ligand backbone on enantioselectivity is shown by entries 1, 2, and 6-8. These reactions were conducted with

several classes of ligands containing the same 3,5-di-*tert*-butyl-4-methoxyphenyl (DTBM) groups. The ligand (**L11**) that contains a 2,2',3,3'-tetrahydro-[5,5'-bibenzo[*b*][1,4]dioxine backbone (SYNPHOS) led to the highest enantioselectivity among a SEGPHOS ligand, a BIPHEP ligand, a SYNPHOS ligand, a garphos ligand, and a BINAP ligand.

Having found that the backbone of SYNPHOS ligands leads to the highest enantioselectivity, we examined reactions catalyzed by copper complexes of (*R*)-TMS-SYNPHOS (**L12**) in more detail. The enantioselectivity of the reaction conducted at room temperature with (*R*)-TMS-SYNPHOS (88:12 er, entry 9) was higher than that with (*R*)-DTBM-SYNPHOS (85:15 er). Reducing the reaction temperature from room temperature to -15 °C increased the enantioselectivity of the reaction with (*R*)-TMS-SYNPHOS further to 92:8 er (entry 10). The reaction conducted with (*R*)-TMG-SYNPHOS (**L13**) that contains 3,5-bis(trimethylgermanyl)phenyl groups proceeded with a higher enantioselectivity than that conducted with TMS-SYNPHOS and was a high 94:6 er at -15 °C (entry 11). This new ligand, (*R*)-TMG-SYNPHOS, formed a catalyst that was particularly active for the reactions of 1,1-disubstituted alkenes, in addition to one that reacts with high enantioselectivity. For comparison, the catalyst formed from (*S*)-DTBM-SEGPHOS was inactive for hydroboration of alkene **3a** at -15 °C (entry 12) whereas the catalyst formed from (*R*)-TMG-SYNPHOS gave the hydroboration product in high yield, as well as high er, at this temperature. A few factors were essential to achieve the high enantioselectivity. First, the catalyst formed from (*R*)-TMG-SYNPHOS that contains large 3,5-bis(trimethylgermanyl)phenyl substituents most effectively differentiates the two prochiral faces of **3a** among the complexes formed from all the ligands examined. Second, the large 3,5-bis(trimethylgermanyl)phenyl sub stituents on the ligand caused the catalyst to be highly active, and this activity allowed the reaction to be conducted at low temperatures.

Scope of the asymmetric hydroboration of 1,1-disubstituted alkenes. Having established conditions for the asymmetric hydroboration, we examined the scope of the asymmetric hydroboration of 1,1-disubstituted alkenes that contain two different primary alkyl groups (Table 2). First, the reactions proceeded with consistently high enantioselectivity with 1,1-alkenes that contain a benzyl group and a primary alkyl group, such as a methyl group (**3a**), an ethyl group (**3b**), a methoxymethyl group (**3c**), a 2-methoxyethoxymethyl group (**3d**), a silyloxymethyl group (**3e**), and a fluoromethyl group (**3f**). Enantioselectivity equal to or higher than 95:5 er was obtained for the reactions of **3b** and **3f**. Second, the reactions of 1,1-alkenes that contain a methyl group and an aryl- or heteroarylmethyl group proceeded with high enantioselectivity when the aryl group was either electron-rich or electron-poor or was a heteroaryl ring, such as pyrimidine (**3i**), indole (**3j**), or benzothiophene (**3k**). The reactions of alkenes containing 6,5-fused electron-rich heterocycles were less enantioselective than those containing electron-poor heterocycles.

Table 2. Scope of enantioselective hydroboration of 1,1-disubstituted alkenes

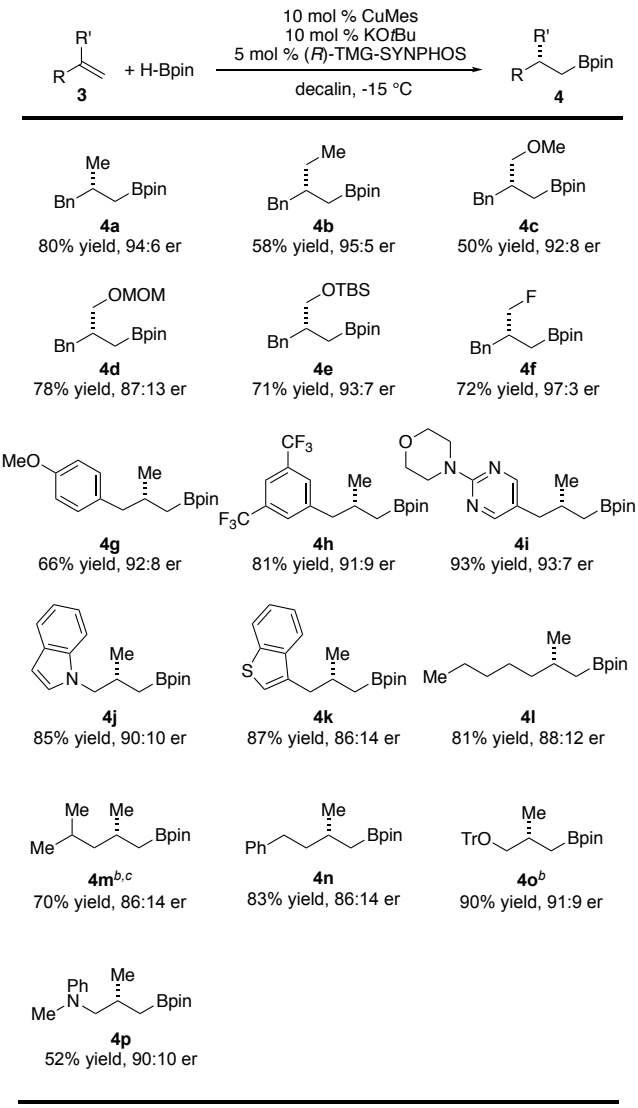

[a]Reaction conditions: **3** (0.2 mmol), HBpin (0.24 mmol, 1.2 equiv), CuMes (10 mol %), KO*t*Bu (10 mol %) and **L13** (5 mol %) in decalin, 72 h, -15 °C; yields refer to those of the isolated products;[b]reactions conducted at -5 °C;[c]3 equivalent of alkene instead of 1 equiv used.

Reactions of alkenes containing a methyl group and a primary alkyl group that is not benzyl also were investigated. In general, the enantioselectivities of these reactions were lower (<90:10 er) than those of the reactions of alkenes **3a**, **3g**, and **3h** just discussed that contain arylmethyl groups, but the enantioselectivities were still substantial. Alkenes containing an sp^3-hybridized carbon containing a substituent at the position β to the alkene (**3m**) were less reactive towards the hydroboration than those lacking a group at this position (**3l**) or those containing an sp^2-hybridized carbon β to the alkene (**3a**). This lower reactivity is likely due to weaker binding of an alkene that contains substituents at this position. Thus, the reaction was conducted at -5 °C instead of -15 °C to obtain the corresponding product in a reasonable yield. Finally, the reaction of alkenes containing a trityl ether moiety (**3o**) and a tertiary amine moiety (**3p**) proceeded with good enantioselectivity.

Although the majority of the hydroborations proceeded in good to high yields, the reactions of a few alkenes (**3b**, **3c**, **3p**) occurred in lower yields at 72 h due to slower reaction rates than those with the majority of the reactions. The absence of side products in these cases implies that the yields would likely be higher at higher loadings of catlayst.

2.2 Computational analysis of the origin of the high enantioselectivity with TMG-substituted bisphosphine ligands. The ascending trend of the calculated $\Delta\Delta G^{\ddagger}$ values in hydrocupration with DTB-, TMS-, and TMG-SEGPHOS ligands (Scheme 2) is consistent with the experimentally observed enantioselectivity shown in Table 1, in which the highest enantioselectivity was obtained with TMG-SYNPHOS as the ligand. To reveal the origin of the improved enantioselectivity with ligands containing trimethylgermanyl groups, we conducted calculations by energy decomposition analysis (EDA) to analyze the different types of ligand-substrate interactions in the transition states for hydrocupration.

Following the approach used in our previous computational studies,[4-5, 15, 38] we dissected the computed activation energies ($\Delta E^{\ddagger}$) into three terms:

$$\Delta E^{\ddagger} = \Delta E_{\text{dist}} + \Delta E_{\text{int-bond}} + \Delta E_{\text{int-space}} \quad (1)$$

ΔE_{dist} is the total energy required to distort the LCuH fragment and the alkene fragment from the ground state into their transition state geometries. $\Delta E_{\text{int-space}}$ is the through-space interaction energy calculated from a supramolecular complex of the bisphosphine ligand and the alkene at the transition state geometry in the absence of the CuH moiety. $\Delta E_{\text{int-bond}}$ is the through-bond interaction energy between the CuH moiety and the alkene. This procedure allows the through-space interaction energy ($\Delta E_{\text{int-space}}$) between the ligand and the substrate to be dissected further using the second-generatioin ALMO-EDA[39-41] method implemented in Q-Chem 5.2:[42]

$$\Delta E_{\text{int-space}} = \Delta E_{\text{Pauli}} + \Delta E_{\text{elstat}} + \Delta E_{\text{orb}} + \Delta E_{\text{disp}} \quad (2)$$

In this equation, ΔE_{Pauli}, ΔE_{elstat}, ΔE_{orb} and ΔE_{disp} are the energies of Pauli repulsions, electrostatic interactions, orbital interactions (*i.e.* polarization and charge transfer), and London dispersion interactions, respectively.

The values for the individual energy terms were computed for all of the six hydrocupration transition states (**TS-1A–TS-3A** and **TS-1B–TS-3B**, Scheme 2) and are provided in Table S1. To identify factors that control the enantioselectivity, we analyzed the difference in each energy term ($\Delta\Delta E$) between pairs of transition states leading to the major (**TS-A**) and minor enantiomeric products (**TS-B**) (Figure 1).

The distortion-interaction analysis (Figure 1A) suggests that the impacts of through-bond interaction ($\Delta\Delta E_{\text{int-bond}}$) on the enantioselectivity are negligible and the through-space interactions ($\Delta\Delta E_{\text{int-space}}$) are the dominant factors that affect the enantioselectivity. In particular, the through-space interactions between the TMS- and TMG-SEGPHOS ligand and the alkene in **TS2A** and **TS3A** are significantly more favorable than those in **TS2B** and **TS3B** ($\Delta\Delta E_{\text{int-space}}$ = 4.7, 4.5 kcal/mol, respectively), while the through-space ligand-substrate interactions of transition state **TS1A** are comparable to those of transition state **TS1B** ($\Delta\Delta E_{\text{int-space}}$ = 1.5 kcal/mol).

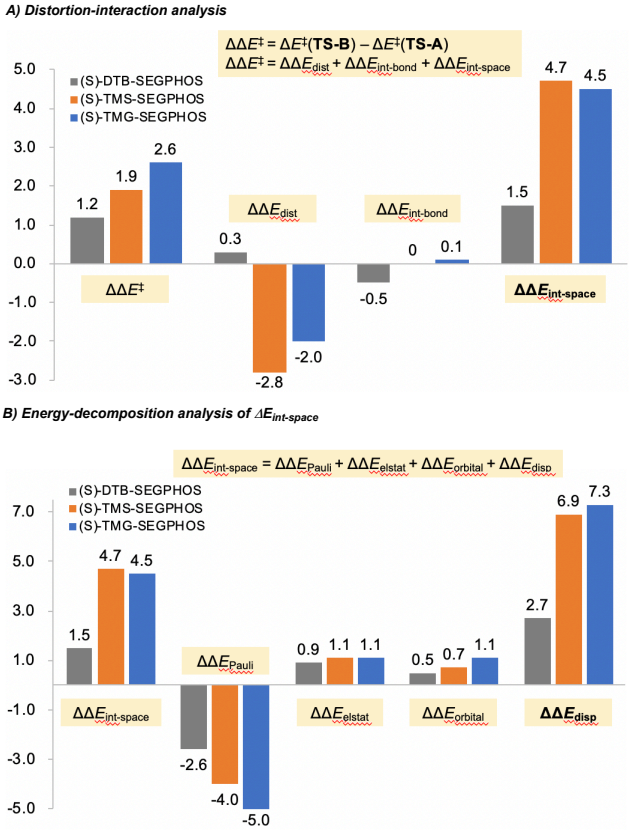

Figure 1. Distortion-interaction analysis and energy decomposition analysis (EDA) to reveal factors that determine the enantioselectivity of olefin hydrocupration. All energies are in kcal/mol.

The EDA calculations (Figure 1B) indicated that the differences between the through-space interaction energies are mainly affected by the attractive London dispersion ($\Delta\Delta E_{\text{disp}}$) and Pauli repulsion terms ($\Delta\Delta E_{\text{Pauli}}$). The influences of electrostatics ($\Delta\Delta E_{\text{elstat}}$) and orbital interactions ($\Delta\Delta E_{\text{orb}}$) on the enantioselectivity are small.

The EDA analysis showed that dispersion is the major interaction that causes the overall $\Delta\Delta E^{\ddagger}$ values to be positive, resulting in a higher enantioselectivity from reactions with the TMG-containing ligands than with the DTB-containing ligands. Specifically, the germanyl-groups, which are larger in volume than *tert*-butyl groups, in TMG-SEGPHOS lead to $\Delta\Delta E_{\text{disp}}$ values (7.3 kcal/mol) that are more than twice the $\Delta\Delta E_{\text{disp}}$ value (2.7 kcal/mol) corresponding to the transition state with the DTB-SEGPHOS ligand.

In contrast, the $\Delta\Delta E_{\text{Pauli}}$ terms are negative, indicating that transition states leading to the major enantiomer of the product (**TS1A–TS3A**) have greater steric repulsions between the ligand and the substrate than those leading to the minor enantiomer (**TS1B–TS3B**). This influence of the steric effect contrasts the typical presumption that the sterically encumbered ligands improve the enantioselectivity of transition metal-catalyzed asymmetric reactions due to increased steric interactions between the ligand and the substrate. Instead, here, the dominant factor controlling the enantioselectivity is the London dispersion interactions between the ligand and the alkene substrate ($\Delta\Delta E_{\text{disp}}$). The attractive dispersion forces in **TS1A–TS3A** completely compensate the disfavored steric repulsions and cause the overall

through-space ligand-substrate interactions to be more favorable and the energy of the transition state to be lower for **TS1A**–**TS3A** than for **TS1B**–**TS3B**.

To obtain further insights into this unusual dispersion-controlled enantioselectivity, we plotted the quadrant diagrams of the transition states for hydrocupration (Figure 2). Conformational analysis of the alkene in the transition states for hydrocupration revealed that the *n*-propyl substituent on the alkene adopts two different conformations in transition states leading to the different enantiomers. Because the 1,1-disubstituted alkene favors the eclipsed conformation to minimize allylic-1,2-interactions,[43-44] the *n*-Pr group can be oriented toward or away from the LCuH catalyst. In the most stable conformers of the transition states leading to the major enantiomer (**TS-1A** and **TS-3A**), the *n*-Pr group points towards the LCuH catalyst. Because the *n*-Pr group in these transition states is in a less occupied quadrant, this conformation allows the alkyl chain to be closer to the ligand and, thus, to have stronger dispersion interactions. On the other hand, the *n*-Pr group in the disfavored transition states (**TS-1B** and **TS-3B**) is in the more occupied quadrant and adopts a different conformation in which it points away from the ligand. Although this conformation leads to a slight decrease in ligand-substrate Pauli repulsions, the dispersion interactions are significantly decreased due to the conformational change in **TS-1B** and **TS-3B**. Thus, the transition states leading to the major enantiomer (**TS-1A** and **TS-3A**) are more stable than those leading to the minor enantiomer (**TS-1B** and **TS-3B**) because the conformation of the substrate in **TS-1A** and **TS-3A** allows more favorable dispersion interactions with the bisphosphine ligand than it does in **TS-1B** and **TS-3B**.

This dispersion effect is sensitive to the size of the 3,5-substituents on the *P*-aryl groups of the ligand. The dispersion interaction between the substrate and TMG-SEGPHOS in **TS-3A** ($\Delta E_{disp} = -26.9$ kcal/mol) is 2.7 kcal/mol stronger than that with the DTB-SEGPHOS ligand in **TS-1A** ($\Delta E_{disp} = -24.2$ kcal/mol). The computed pairwise dispersion interaction energies between each of the *t*-Bu/TMG substituents and the alkene substrate revealed stabilizing interactions with multiple TMG substituents in **TS-3A** that are all slightly stronger than the corresponding dispersion interactions with *t*-Bu groups in **TS-1A**. In contrast, in the transition states leading to the minor enantiomer, **TS-3B** with the TMG-SEGPHOS ligand has a smaller dispersion energy than **TS-1B** with DTB-SEGPHOS ($\Delta E_{disp} = -19.6$ and -21.5 kcal/mol respectively). This is in part due to the conformation of the alkene, which points the *n*-Pr group away from the ligand. In addition, the bulky TMG substituents decrease the conformational flexibility of the *P*-aryl groups and lead to a longer CH–π distance between the *n*-Pr and *P*-aryl group (3.43 Å) in **TS-3B** than that in **TS-1B** (2.71 Å).

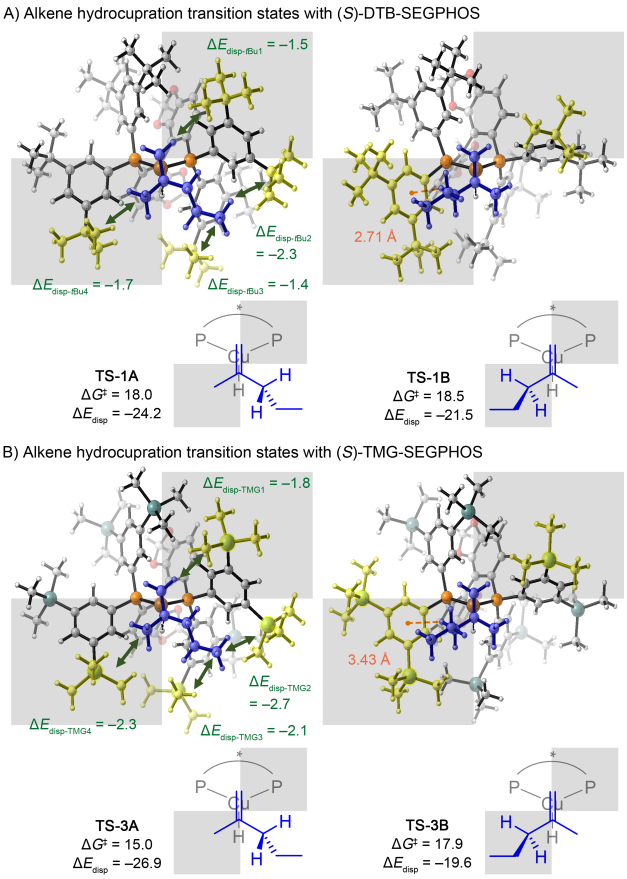

Figure 2. Optimized structures of alkene hydrocupration transition states. The pairwise dispersion interactions between alkene and the highlighted *t*-Bu or TMG substituents of ligands in **TS-1A** and **TS-3A** are shown in kcal/mol. The CH–π distances in **TS-1B** and **TS-3B** are given in orange.

Overall, the EDA calculations show that ligand-substrate dispersion interactions constitute the dominant factor that controls the enantioselectivity. Bulkier substituents at the 3,5-positions of the *P*-aryl groups of the ligand enhance the ligand-substrate dispersion interaction (ΔE_{disp}) in the favored transition state (*e.g.* **TS-3A**) and weaken the dispersion in the disfavored transition state (*e.g.* **TS-3B**). In addition, the computational results corroborate our experimental finding that ligands containing larger 3,5-substituents led to a higher catalytic activity than those containing smaller substituents. The EDA calculations indicate that the reactivity enhancement is also due to the greater stabilizing dispersion interactions in the transition states ligated with TMG-SEGPHOS (see Supporting Information for more detailed discussions on factors controlling reactivity). These analyses highlight the importance of understanding non-covalent ligand-substrate interactions to enhance reactivity and selectivity of transition metal-catalyzed reactions and show how the use of main group elements in the design of ligands can enhance these intereactions.

2.3 Development of hydroboration of unactivated 1,2-disubstituted alkenes. Having observed a significant increase in the activity and selectivity of the copper catalyst for the hydroboration of 1,1-disubstituted alkenes, we tested whether ligands that contain trimethylgermanyl groups would also enhance the rate

of the hydroboration of alkenes that have generally undergone metal-catalyzed hydroboration with low rates.

Many catalysts promote the hydroboration of nonconjugated internal alkenes, but catalysts that directly add B-H bonds across such alkene double bonds without chain-walking isomerization[45-53] are rare.[54-55] The rarity of such catalysts is due to faster β-hydrogen elimination from the secondary alkylmetal species formed by insertion of the internal alkene than from the corresponding primary alkylmetal species.[56]

Previously, we showed that the reactions of internal alkenes bearing electron-withdrawing groups β to the alkene moiety occurred in high yield and without the formation of side products resulting from chain-walking processes. However, the reactions of unactivated 1,2-disubstituted alkenes required a large excess of alkenes and proceeded in lower yields than did reactions of nonconjugated 1,2-disubstituted alkenes that are electronically activated.[55] Our previous mechanistic study showed that the reactions of 1,2-disubstituted alkenes is inverse-order in [HBpin] and positive-order in [alkene] and that the olefin insertion is the rate-limiting step.[31] Thus, if a ligand that increases the rate of alkene insertion could be identified, then the reaction of unactivated 1,2-disubstituted alkenes might proceed in high yields and the need for excess of such alkenes could be eliminated.

Scheme 4. Synthesis of DTMSM-SEGPHOS (L14) and DTMGM-SEGPHOS (L15)

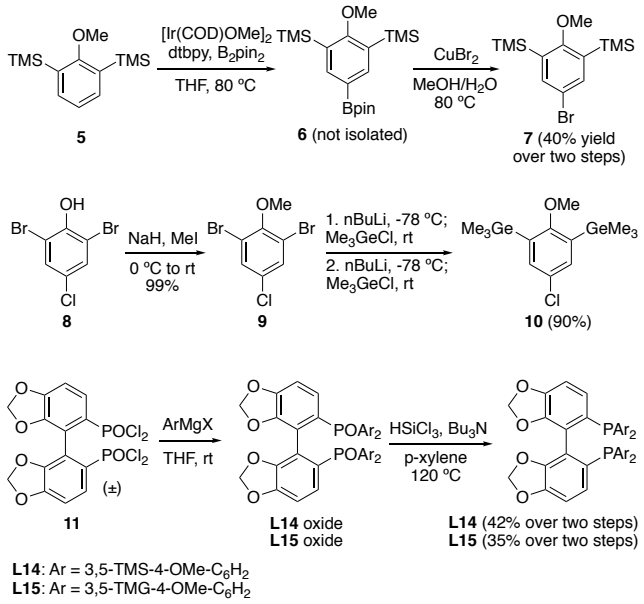

Synthesis of DTMSM-SEGPHOS and DTMGM-SEGPHOS. To test the effect of silyl and germanyl substituents on the rate of reactions of 1,2-disubstituted alkenes, we prepared two new ligands, DTMSM-SEGPHOS (L14) and DTMGM-SEGPHOS (L15), which contain 3,5-bis(trimethylsilyl)-4-methoxyphenyl groups and 3,5-bis(trimethylgermanyl)-4-methoxyphenyl groups, respectively. Previously in this paper we showed that the catalysts formed from ligands that contain trimethylgermanyl groups at the 3- and 5-positions of the phenyl group on the phosphorus are more active for copper-catalyzed hydroboration than those formed from ligands that have trimethylsilyl or tert-butyl groups at the 3- and 5-positions.

The synthetic route to DTMSM-SEGPHOS and DTMGM-SEGPHOS is depicted in Scheme 4. Analogous to the synthesis shown in Scheme 3, these two ligands were assembled by the reaction between the bisphosphonic dichloride (**11**) and the Grignard reagent derived from the corresponding aryl bromide. However, the corresponding aryl bromides for the 3,5-substituted 4-methoxyaryl ligands could not be synthesized by sequential lithium-halogen exchange reactions of 2,4,6-tribromoanisole, which was used for the synthesis of 3,5-bis(trimethylgermanyl)phenyl bromide and 3,5-bis(trimethylsilyl)phenyl bromide,[35] because the exchange reaction on the tribromoanisole was not sufficiently selective for the positions ortho to the methoxy group.

Instead, 3,5-bis(trimethylsilyl)-4-methoxyphenyl bromide (**5**) was prepared by a sequence consisting of C-H borylation and bromination, which was developed by our group.[57] Starting with 2,6-bis(trimethylsilyl)anisole (**6**), the iridium-catalyzed C-H borylation occurred with complete *para*-selectivity to afford 2,6-bis(trimethylsilyl)-4-(pinacolato)boryl anisole (**7**), which was used as a crude material in the subsequent copper-mediated bromination to afford the aryl bromide in 40% overall yield.

However, when we used the same procedure for the synthesis of 3,5-bis(trimethylgermanyl)-4-methoxyphenyl bromide, we observed the formation of degermanylation products that were inseparable from the desired bromination product. Therefore, we prepared 3,5-bis(trimethylgermanyl)-4-methoxyphenyl chloride (**9**) from 2,6-dibromo-4-chlorophenol (**8**). Methylation of **8** proceeded in quantitative yield to afford 2,6-dibromo-4-chloroanisole (**9**). The carbon-bromine bonds in **9** were converted to C-$GeMe_3$ bonds by a sequence of lithium-halogen exchange reactions and germanylation, while the carbon-chlorine bond remained intact. Overall, chloride **10** was obtained in 90% yield over two steps from 2,6-dibromo-4-chlorophenol (**8**).

With bromide **7** and chloride **10** prepared in multigram scale, DTMSM-SEGPHOS and DTMGM-SEGPHOS were synthesized in two steps in 35-42% yield, respectively. The racemic forms of these ligands were used to evaluate the effect of substituents on reaction rate and conversion. We did not attempt to resolve the enantiomers of these ligands to access the enantioenriched samples.

Effects of the ligands on catalyst activity. To determine the effect of the TMS and TMG substituents on the reactivity of the copper catalyst for hydroboration of internal alkenes, we conducted the hydroboration reactions of *trans*-4-octene with the catalysts formed from the ligand used in previous studies,[55] DTBM-SEGPHOS (**L4**), and the two ligands introduced in this work, DTMSM-SEGPHOS (**L14**), and DTMGM-SEGPHOS (**L15**). These data are summarized in Table 3. The reactions were conducted with Cu(*t*BuCN)$_2$OTf, a copper salt reported by our group,[58] as the copper source. The catalyst formed from Cu(*t*BuCN)$_2$OTf was more active than that formed from CuCl, which was used previously.[55, 59] This change allowed the reaction to be evaluated with only 1.2 equivalents of alkene, instead of the 3 equivalents of alkene used in earlier studies.

Table 3. Evaluation of ligands for hydroboration of unactivated internal alkene 12 [a]

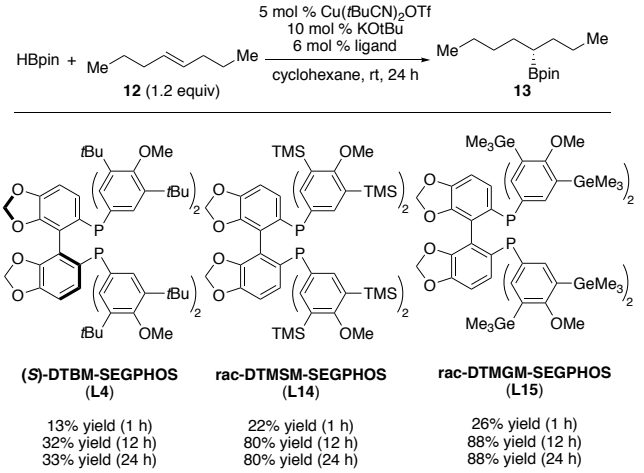

[a]Reaction conditions: **12** (0.24 mmol, 1.2 equiv), HBpin (0.2 mmol, 1 equiv), Cu(*t*BuCN)$_2$OTf (5 mol %), KO*t*Bu (10 mol %), and ligand (6 mol %) in cyclohexane, rt, 24 h.

We found that reactions conducted with catalysts derived from DTMSM-SEGPHOS, and DTMGM-SEGPHOS reacted faster and in higher yield (>80% yield) than did that with DTBM-SEGPHOS (33% yield). The reactions with the catalyst containing DTBM-SEGPHOS as ligand stopped after 12 hours, presumably due to catalyst decomposition. These results suggest that the catalysts ligated by DTMSM-SEGPHOS, and DTMGM-SEGPHOS are more reactive towards insertion of unactivated internal alkenes than that ligated by DTBM-SEGPHOS.

3. CONCLUSION

In conclusion, we have developed two new ligands that contain trimethylgermanyl groups at the 3- and 5-positions of the phosphine-bound aryl ring and applied these ligands to the copper-catalyzed hydroboration of alkenes. The enantioselectivity of the reactions of 1,1-disubstituted alkenes that contain two primary alkyl groups catalyzed by the copper complex derived from (*R*)-TMG-SYNPHOS is significantly higher than that of these reactions with prior catalysts. This higher enantioselectivity results from improved differentiation of the two primary alkyl groups on the alkene by the catalyst ligated by bisphosphines that contain bulky groups at the 3- and 5-positions of the phenyl ring at phosphorus. The modification of existing ligands containing these bulky germanium-containing groups also substantially enhances the activity of the copper catalyst toward hydroboration. The catalyst ligated by DTMGM-SEGPHOS is particularly active toward the hydroboration of unactivated internal alkenes. The high activity of the catalyst allowed the reaction to be conducted with 1.2 equivalents of alkene, which is sufficiently lower than the 3 equivalents required by previous methods. DFT calculations revealed that the improved enantioselectivity of the reaction and higher catalytic activity of the copper catalysts derived from these trimethylgermanyl-containing ligands resulted from attractive dispersion interactions between the bulky germanium-containing groups and the substrate. We anticipate that the unique properties and the facile synthesis of these two ligands containing trimethylgermanyl groups would lead to applications in other transition-metal-catalyzed reactions.

ASSOCIATED CONTENT

Supporting Information

The Supporting Information is available free of charge on the ACS Publications website.

Experimental procedures, characterization data, Cartesian coordinates for all computed structures (PDF)

AUTHOR INFORMATION

Corresponding Author

*jhartwig@berkeley.edu
*pengliu@pitt.edu

ACKNOWLEDGMENT

This work was supported by the Director, Office of Science, of the U.S. Department of Energy under contract No. DE-AC02-05CH11231. P.L. and X.Q. thank the University of Pittsburgh and the NIH (R35GM128779) for financial support of the computational work. DFT calculations were conducted in the Molecular Graphics and Computation Facility at UC Berkeley (NSF CHE-0840505) and the Center for Research Computing at the University of Pittsburgh, and the Extreme Science and Engineering Discovery Environment (XSEDE), and the TACC Frontera Supercomputer. We thank Takasago for gifts of (*S*)-DTBM-SEGPHOS. Y.X. thanks Bristol-Myers Squibb for a graduate fellowship.

REFERENCES

1. Walsh, P. J.; Kozlowski, M. C., Fundamentals of Asymmetric Catalysis. University Science Books: Sausalito, CA, 2009; p 114.
2. Saito, T.; Yokozawa, T.; Ishizaki, T.; Moroi, T.; Sayo, N.; Miura, T.; Kumobayashi, H., New Chiral Diphosphine Ligands Designed to have a Narrow Dihedral Angle in the Biaryl Backbone. *Adv. Synth. Cat.* **2001,** *343*, 264-267.
3. Lipshutz, B. H.; Noson, K.; Chrisman, W.; Lower, A., Asymmetric Hydrosilylation of Aryl Ketones Catalyzed by Copper Hydride Complexed by Nonracemic Biphenyl Bis-phosphine Ligands. *J. Am. Chem. Soc.* **2003,** *125*, 8779-8789.
4. Lu, G.; Liu, R. Y.; Yang, Y.; Fang, C.; Lambrecht, D. S.; Buchwald, S. L.; Liu, P., Ligand–Substrate Dispersion Facilitates the Copper-Catalyzed Hydroamination of Unactivated Olefins. *J. Am. Chem. Soc.* **2017,** *139*, 16548-16555.
5. Thomas, A. A.; Speck, K.; Kevlishvili, I.; Lu, Z.; Liu, P.; Buchwald, S. L., Mechanistically Guided Design of Ligands That Significantly Improve the Efficiency of CuH-Catalyzed Hydroamination Reactions. *J. Am. Chem. Soc.* **2018,** *140*, 13976-13984.
6. Liptrot, D. J.; Power, P. P., London dispersion forces in sterically crowded inorganic and organometallic molecules. *Nat. Rev. Chem.* **2017,** *1*, 0004.
7. Wagner, J. P.; Schreiner, P. R., London Dispersion in Molecular Chemistry—Reconsidering Steric Effects. *Angew. Chem. Int. Ed.* **2015,** *54*, 12274-12296.
8. Wolters, L. P.; Koekkoek, R.; Bickelhaupt, F. M., Role of Steric Attraction and Bite-Angle Flexibility in Metal-Mediated C–H Bond Activation. *ACS Catal.* **2015,** *5*, 5766-5775.
9. Lyngvi, E.; Sanhueza, I. A.; Schoenebeck, F., Dispersion Makes the Difference: Bisligated Transition States Found for the Oxidative Addition of Pd(PtBu3)2 to Ar-OSO2R and Dispersion-Controlled Chemoselectivity in Reactions with Pd[P(iPr)(tBu2)]2. *Organometallics* **2015,** *34*, 805-812.
10. Chen, J.; Zhang, Z.; Li, B.; Li, F.; Wang, Y.; Zhao, M.; Gridnev, I. D.; Imamoto, T.; Zhang, W., Pd(OAc)2-catalyzed asymmetric hydrogenation of sterically hindered N-tosylimines. *Nat. Comm.* **2018,** *9*, 5000.

11. Kalvet, I.; Deckers, K.; Funes-Ardoiz, I.; Magnin, G.; Sperger, T.; Kremer, M.; Schoenebeck, F., Selective ortho-Functionalization of Adamantylarenes Enabled by Dispersion and an Air-Stable Palladium(I) Dimer. *Angew. Chem. Int. Ed.* **2020,** *59*, 7721-7725.

12. Saper, N. I.; Ohgi, A.; Small, D. W.; Semba, K.; Nakao, Y.; Hartwig, J. F., Nickel-catalysed anti-Markovnikov hydroarylation of unactivated alkenes with unactivated arenes facilitated by non-covalent interactions. *Nat. Chem.* **2020,** *12*, 276-283.

13. Gridnev, I. D., Attraction versus Repulsion in Rhodium-Catalyzed Asymmetric Hydrogenation. *ChemCatChem* **2016,** *8*, 3463-3468.

14. Chen, J.; Gridnev, I. D., Size is Important: Artificial Catalyst Mimics Behavior of Natural Enzymes. *iScience* **2020,** *23*, 100960.

15. Deng, L.; Fu, Y.; Lee, S. Y.; Wang, C.; Liu, P.; Dong, G., Kinetic Resolution via Rh-Catalyzed C–C Activation of Cyclobutanones at Room Temperature. *J. Am. Chem. Soc.* **2019,** *141*, 16260-16265.

16. Iwamoto, H.; Endo, K.; Ozawa, Y.; Watanabe, Y.; Kubota, K.; Imamoto, T.; Ito, H., Copper(I)-Catalyzed Enantioconvergent Borylation of Racemic Benzyl Chlorides Enabled by Quadrant-by-Quadrant Structure Modification of Chiral Bisphosphine Ligands. *Angew. Chem. Int. Ed.* **2019,** *58*, 11112-11117.

17. Neel, A. J.; Hilton, M. J.; Sigman, M. S.; Toste, F. D., Exploiting non-covalent π interactions for catalyst design. *Nature* **2017,** *543*, 637.

18. Straker, R. N.; Peng, Q.; Mekareeya, A.; Paton, R. S.; Anderson, E. A., Computational ligand design in enantio- and diastereoselective ynamide [5+2] cycloisomerization. *Nat. Comm.* **2016,** *7*, 10109.

19. Power, P. P., Main-group elements as transition metals. *Nature* **2010,** *463*, 171-177.

20. Chen, J.; Xi, T.; Lu, Z., Iminopyridine Oxazoline Iron Catalyst for Asymmetric Hydroboration of 1,1-Disubtituted Aryl Alkenes. *Org. Lett.* **2014,** *16*, 6452-6455.

21. Chen, J.; Xi, T.; Ren, X.; Cheng, B.; Guo, J.; Lu, Z., Asymmetric cobalt catalysts for hydroboration of 1,1-disubstituted alkenes. *Org. Chem. Front* **2014,** *1*, 1306-1309.

22. Zhang, L.; Zuo, Z.; Wan, X.; Huang, Z., Cobalt-Catalyzed Enantioselective Hydroboration of 1,1-Disubstituted Aryl Alkenes. *J. Am. Chem. Soc.* **2014,** *136*, 15501-15504.

23. Thomas, S. P.; Aggarwal, V. K., Asymmetric Hydroboration of 1,1-Disubstituted Alkenes. *Angew. Chem. Int. Ed.* **2009,** *48*, 1896-1898.

24. Jang, W. J.; Song, S. M.; Moon, J. H.; Lee, J. Y.; Yun, J., Copper-Catalyzed Enantioselective Hydroboration of Unactivated 1,1-Disubstituted Alkenes. *J. Am. Chem. Soc.* **2017,** *139*, 13660-13663.

25. Teo, W. J.; Ge, S., Cobalt-Catalyzed Enantioselective Synthesis of Chiral gem-Bis(boryl)alkanes. *Angew. Chem. Int. Ed.* **2018,** *57*, 12935-12939.

26. Chen, J.; Lu, Z., Asymmetric hydrofunctionalization of minimally functionalized alkenes via earth abundant transition metal catalysis. *Org. Chem. Front* **2018,** *5*, 260-272.

27. Zhu, S.; Buchwald, S. L., Enantioselective CuH-Catalyzed Anti-Markovnikov Hydroamination of 1,1-Disubstituted Alkenes. *J. Am. Chem. Soc.* **2014,** *136*, 15913-15916.

28. Chen, J.; Cheng, B.; Cao, M.; Lu, Z., Iron-Catalyzed Asymmetric Hydrosilylation of 1,1-Disubstituted Alkenes. *Angew. Chem. Int. Ed.* **2015,** *54*, 4661-4664.

29. Deng, Y.; Wang, H.; Sun, Y.; Wang, X., Principles and Applications of Enantioselective Hydroformylation of Terminal Disubstituted Alkenes. *ACS Catal.* **2015,** *5*, 6828-6837.

30. Lu, Z.; Buchwald, S. L., Enantioselective Preparation of Arenes with β-Stereogenic Centers: Confronting the 1,1-Disubstituted Olefin Problem Using CuH/Pd Cooperative Catalysis. *Angew. Chem. Int. Ed.* **2020,** *59*, 16128-16132.

31. Xi, Y.; Hartwig, J. F., Mechanistic Studies of Copper-Catalyzed Asymmetric Hydroboration of Alkenes. *J. Am. Chem. Soc.* **2017,** *139*, 12758-12772.

32. Zhang, Q.-W.; An, K.; Liu, L.-C.; Yue, Y.; He, W., Rhodium-Catalyzed Enantioselective Intramolecular C□H Silylation for the Syntheses of Planar-Chiral Metallocene Siloles. *Angew. Chem. Int. Ed.* **2015,** *54*, 6918-6921.

33. Zhang, Q.-W.; An, K.; Liu, L.-C.; Zhang, Q.; Guo, H.; He, W., Construction of Chiral Tetraorganosilicons by Tandem Desymmetrization of Silacyclobutanes/Intermolecular Dehydrogenative Silylation. *Angew. Chem. Int. Ed.* **2017,** *56*, 1125-1129.

34. Berhal, F.; Esseiva, O.; Martin, C.-H.; Tone, H.; Genet, J.-P.; Ayad, T.; Ratovelomanana-Vidal, V., (R)-3,5-diCF3-SYNPHOS and (R)-p-CF3-SYNPHOS, Electron-Poor Diphosphines for Efficient Room Temperature Rh-Catalyzed Asymmetric Conjugate Addition of Arylboronic Acids. *Org. Lett.* **2011,** *13*, 2806-2809.

35. Sevov, C. S.; Hartwig, J. F., Iridium-Catalyzed Oxidative Olefination of Furans with Unactivated Alkenes. *J. Am. Chem. Soc.* **2014,** *136*, 10625-10631.

36. See Supporting Information for details

37. See Supporting Information for discussions.

38. Qi, X.; Kohler, D. G.; Hull, K. L.; Liu, P., Energy Decomposition Analyses Reveal the Origins of Catalyst and Nucleophile Effects on Regioselectivity in Nucleopalladation of Alkenes. *J. Am. Chem. Soc.* **2019,** *141*, 11892-11904.

39. Horn, P. R.; Head-Gordon, M., Polarization contributions to intermolecular interactions revisited with fragment electric-field response functions. *J Chem Phys* **2015,** *143*, 114111.

40. Horn, P. R.; Mao, Y.; Head-Gordon, M., Probing non-covalent interactions with a second generation energy decomposition analysis using absolutely localized molecular orbitals. *Phys. Chem. Chem. Phys.* **2016,** *18*, 23067-79.

41. Horn, P. R.; Mao, Y.; Head-Gordon, M., Defining the contributions of permanent electrostatics, Pauli repulsion, and dispersion in density functional theory calculations of intermolecular interaction energies. *J. Chem. Phys.* **2016,** *144*, 114107.

42. Shao, Y.; Gan, Z.; Epifanovsky, E.; Gilbert, A. T. B.; Wormit, M.; Kussmann, J.; Lange, A. W.; Behn, A.; Deng, J.; Feng, X.; Ghosh, D.; Goldey, M.; Horn, P. R.; Jacobson, L. D.; Kaliman, I.; Khaliullin, R. Z.; Kuś, T.; Landau, A.; Liu, J.; Proynov, E. I.; Rhee, Y. M.; Richard, R. M.; Rohrdanz, M. A.; Steele, R. P.; Sundstrom, E. J.; Woodcock, H. L.; Zimmerman, P. M.; Zuev, D.; Albrecht, B.; Alguire, E.; Austin, B.; Beran, G. J. O.; Bernard, Y. A.; Berquist, E.; Brandhorst, K.; Bravaya, K. B.; Brown, S. T.; Casanova, D.; Chang, C.-M.; Chen, Y.; Chien, S. H.; Closser, K. D.; Crittenden, D. L.; Diedenhofen, M.; DiStasio, R. A.; Do, H.; Dutoi, A. D.; Edgar, R. G.; Fatehi, S.; Fusti-Molnar, L.; Ghysels, A.; Golubeva-Zadorozhnaya, A.; Gomes, J.; Hanson-Heine, M. W. D.; Harbach, P. H. P.; Hauser, A. W.; Hohenstein, E. G.; Holden, Z. C.; Jagau, T.-C.; Ji, H.; Kaduk, B.; Khistyaev, K.; Kim, J.; Kim, J.; King, R. A.; Klunzinger, P.; Kosenkov, D.; Kowalczyk, T.; Krauter, C. M.; Lao, K. U.; Laurent, A. D.; Lawler, K. V.; Levchenko, S. V.; Lin, C. Y.; Liu, F.; Livshits, E.; Lochan, R. C.; Luenser, A.; Manohar, P.; Manzer, S. F.; Mao, S.-P.; Mardirossian, N.; Marenich, A. V.; Maurer, S. A.; Mayhall, N. J.; Neuscamman, E.; Oana, C. M.; Olivares-Amaya, R.; O'Neill, D. P.; Parkhill, J. A.; Perrine, T. M.; Peverati, R.; Prociuk, A.; Rehn, D. R.; Rosta, E.; Russ, N. J.; Sharada, S. M.; Sharma, S.; Small, D. W.; Sodt, A.; Stein, T.; Stück, D.; Su, Y.-C.; Thom, A. J. W.; Tsuchimochi, T.; Vanovschi, V.; Vogt, L.; Vydrov, O.; Wang, T.; Watson, M. A.; Wenzel, J.; White, A.; Williams, C. F.; Yang, J.; Yeganeh, S.; Yost, S. R.; You, Z.-Q.; Zhang, I. Y.; Zhang, X.; Zhao, Y.; Brooks, B. R.; Chan, G. K. L.; Chipman, D. M.; Cramer, C. J.; Goddard, W. A.; Gordon, M. S.; Hehre, W. J.; Klamt, A.; Schaefer, H. F.; Schmidt, M. W.; Sherrill, C. D.; Truhlar, D. G.; Warshel, A.; Xu, X.; Aspuru-Guzik, A.; Baer, R.; Bell, A. T.; Besley, N. A.; Chai, J.-D.; Dreuw, A.; Dunietz, B. D.; Furlani, T. R.; Gwaltney, S. R.; Hsu, C.-P.; Jung, Y.; Kong, J.; Lambrecht, D. S.; Liang, W.; Ochsenfeld, C.; Rassolov, V. A.; Slipchenko, L. V.; Subotnik, J. E.; Van Voorhis, T.; Herbert, J. M.; Krylov, A. I.; Gill, P. M. W.; Head-Gordon, M., Advances in molecular quantum chemistry contained in the Q-Chem 4 program package. *Mol. Phys.* **2014,** *113*, 184-215.

43. McCullough, J. P.; Scott, D. W., Thermodynamic Properties, Vibrational Assignment and Rotational Conformations of 2-Methyl-1-butene. *J. Am. Chem. Soc.* **1959,** *81*, 1331-1334.

44. Hoffmann, R. W., Allylic 1,3-strain as a controlling factor in stereoselective transformations. *Chem. Rev.* **1989,** *89*, 1841-1860.

45. Obligacion, J. V.; Chirik, P. J., Bis(imino)pyridine Cobalt-Catalyzed Alkene Isomerization–Hydroboration: A Strategy for Remote Hydrofunctionalization with Terminal Selectivity. *J. Am. Chem. Soc.* **2013,** *135*, 19107-19110.

46. Lata, C. J.; Crudden, C. M., Dramatic Effect of Lewis Acids on the Rhodium-Catalyzed Hydroboration of Olefins. *J. Am. Chem. Soc.* **2010,** *132*, 131-137.

47. Pereira, S.; Srebnik, M., Transition Metal-Catalyzed Hydroboration of and CCl4 Addition to Alkenes. *J. Am. Chem. Soc.* **1996,** *118*, 909-910.

48. Pereira, S.; Srebnik, M., A study of hydroboration of alkenes and alkynes with pinacolborane catalyzed by transition metals. *Tetrahedron Lett.* **1996,** *37*, 3283-3286.

49. Chen, X.; Cheng, Z.; Guo, J.; Lu, Z., Asymmetric remote C-H borylation of internal alkenes via alkene isomerization. *Nat. Comm.* **2018,** *9*, 3939.

50. Obligacion, J. V.; Chirik, P. J., Highly Selective Bis(imino)pyridine Iron-Catalyzed Alkene Hydroboration. *Org. Lett.* **2013,** *15*, 2680-2683.

51. Ruddy, A. J.; Sydora, O. L.; Small, B. L.; Stradiotto, M.; Turculet, L., (N-Phosphinoamidinate)cobalt-Catalyzed Hydroboration: Alkene Isomerization Affords Terminal Selectivity. *Chem. Eur. J.* **2014,** *20*, 13918-13922.

52. Palmer, W. N.; Diao, T.; Pappas, I.; Chirik, P. J., High-Activity Cobalt Catalysts for Alkene Hydroboration with Electronically Responsive Terpyridine and α-Diimine Ligands. *ACS Catal.* **2015,** *5*, 622-626.

53. Scheuermann, M. L.; Johnson, E. J.; Chirik, P. J., Alkene Isomerization–Hydroboration Promoted by Phosphine-Ligated Cobalt Catalysts. *Org. Lett.* **2015,** *17*, 2716-2719.

54. Smith, S. M.; Thacker, N. C.; Takacs, J. M., Efficient Amide-Directed Catalytic Asymmetric Hydroboration. *J. Am. Chem. Soc.* **2008,** *130*, 3734-3735.

55. Xi, Y.; Hartwig, J. F., Diverse Asymmetric Hydrofunctionalization of Aliphatic Internal Alkenes through Catalytic Regioselective Hydroboration. *J. Am. Chem. Soc.* **2016,** *138*, 6703-6706.

56. Hartwig, J. F., *Organotransition Metal Chemistry, from Bonding to Catalysis*. University Science Books: New York, 2010.

57. Murphy, J. M.; Liao, X.; Hartwig, J. F., Meta Halogenation of 1,3-Disubstituted Arenes via Iridium-Catalyzed Arene Borylation. *J. Am. Chem. Soc.* **2007,** *129*, 15434-15435.

58. Fier, P. S.; Hartwig, J. F., Copper-Mediated Fluorination of Aryl Iodides. *J. Am. Chem. Soc.* **2012,** *134*, 10795-10798.

59. Noh, D.; Chea, H.; Ju, J.; Yun, J., Highly Regio- and Enantioselective Copper-Catalyzed Hydroboration of Styrenes. *Angew. Chem. Int. Ed.* **2009,** *48*, 6062-6064.

Insert Table of Contents artwork here